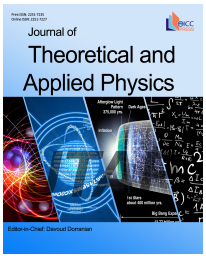

Volume 19, Issue 1, 192514 (1-11)

Journal of Theoretical and Applied Physics (JTAP)

https://doi.org/10.57647/j.jtap.2025.1901.14

Synergistic Cr:Au core shell nanoparticles combination with Paclitaxel (Taxanes) chemo drug on MDA breast cancer cells

Ola F. Al-Salmani[1], Ban H. Adil[2,*], Estabraq A. R. Al-Wasiti[3]

[1]*Ministry of Health, Baghdad Health Department - Al-Karkh, Technical Affairs Department, Laboratory Division, Baghdad, Iraq.*
[2]*Department of Physics, College of Science for Women, University of Baghdad, Baghdad, Iraq.*
[3]*Department of Chemistry and Biochemistry, College of Medicine, Al-Nahrain University, Baghdad, Iraq.*

[*]**Corresponding authors:** banha_phys@csw.uobaghdad.edu.iq

Original Research

Received:
2 October 2024
Revised:
10 December 2024
Accepted:
16 January 2025
Published online:
10 February 2025

Abstract:

Dilute wild thyme extraction was synthesized onto Chrome as a core and the core-shell formed when coated with gold by using the green-plasma jet technique. Nanoparticles created in various ratios (1:9, 2:8, 3:7). Consistent results were obtained during the examination of nanoparticles by UV examination, XRD , SEM and TEM, In addition to measuring the rate of cytotoxicity for Chrome@gold core-shell Nps and Chrme@gold core-shell Nps combined with 25 µg, 50 µg, 100 µg of taxans chemo therapy on breast cancer cell line (MDA) and in the normal cells line (REF) and The best results was after 72 hours, where is the maximum rate of toxicity was in 100% concentration of NPs and the least toxicity was in 25% of NPs.

Keywords: Cr:Au core shell Nps; Plasma jet; MDA; REF; *In vitro* research; Taxanes chemo drug; Synergism

1. Introduction

The most common disease in women, breast cancer (BC), is brought on by malignant lesions in the ductal epithelium. Approximately 500,000 fatalities are attributed to breast cancer each year, affecting 1 in eight to ten women worldwide. Survival from breast cancer rates differ dramatically among industrialized and underdeveloped countries. Breast cancer patients in affluent countries have a 5-year survival rate of up to 80%. In developing nations, individuals with breast cancer have a 5-year survival rate of less than 40%, according to limited statistics [1]. The prevalence of breast cancer is steady worldwide. By 2021, breast cancer is expected to grow by eighty-five incidences each 100,000 females [2]. Knowing that cancer of breasts exists is crucial. affects both men and women. In 2011, the United States had around 2,140 male breast cancer patients, accounting for one percentage of the total instances in existence [3]. Breast cancer is mostly caused by

1. Reproductive variables include breastfeeding status, early menarche, delayed menopause, and nullity.
2. Genetic factors: If a woman's mother has breast cancer, her own chance of developing the disease increases double.
3. Obesity, smoking, and alcohol consumption have been linked to breast cancer development.
4. Long-term exposure to exogenous estrogen also raises the danger cancer of the breast [4].

Currently, chemotherapy and surgical excision are used to treat breast cancer. However, because surgical removal carries a significant psychological burden, the majority of patients chose therapy [5]. Chemotherapeutic drugs are greatly toxic and cannot be reduced using typical pharmaceutical dosage forms, leading to significant adverse effects. Conventional pharmaceuticals lack tumor targeting activity, resulting in just a minimal amount of medications reaching tumor tissues once in the systemic circulation. As a result,

the drug usage rate for typical pharmaceutical preparations is poor. Choosing effective and appropriate medications is crucial for treating breast cancer. Nano-drug delivery methods offer lower toxicity and better bioavailability, making them a popular study topic [6]. Nano-drug delivery systems Nanoparticles, Nano capsules are the most common types. Nano-medication delivery mechanisms allow pharmaceuticals to be dispersed, absorption, and linked covalently to nanocarrier surfaces, or encapsulated and embedded. This not only improves medication solubility and usage in living systems, but likewise target the cancer location by leveraging the solid tumors' high permeability and retention and adding apparent changes in the transporter. This reduces medication waste during translocation to regular tissues and improves treatment protection [7]. Nano-medication delivery technologies offer precision targeting, lower toxicity, and increased drug availability, making them effective for medical diagnosis and therapy. Nano-medication delivery mechanisms have been shown to effectively transport chemotherapeutic medications to tumor locations, making them an excellent therapy option for breast cancer [8]. Stable colloids with dimensions ranging from $(1-1000)$ nm are called nanoparticles. Medicines are dissolved and encapsulated in polymeric materials to form nanoparticles. Nanoparticles can be classified into two types: those with a film-shell and those with a robust framework which stores drugs. Nanoparticles are advantageous carriers for anticancer medicines. Benefits of this approach include reduced toxicity, better solubility, longer retention duration at the tumor location, higher bioavailability, and accurate targeting. Nanoparticles accumulate preferentially in the tumor site due to its physiological properties. High medication concentration at the tumor location enhances effectiveness and minimizes nonspecific adversarial events through chemotherapy. There is a lot of promise for tumor therapy when anticancer medications are delivered using nanoparticles. Extensive research on the use of nanoparticles in breast cancer treatment as a nanodrug delivery method have been conducted with the last 2 years. However, because nanoparticles are generated from a wide range of materials with applications and varying properties, this can lead to a variety of faults and difficulties [9]. The creation of nanoparticles utilizing plants as a precursor has received a lot of attention recently. Green synthesis of nanoparticles using plants is a cost-effective, environmentally friendly, and scalable alternative to traditional chemical and physical approaches [10]. Plasma used to generate and modify nanoparticles. The fourth state of material is plasma, a quasineutral gas made up of cooperatively operating charged and neutral particles. Dissociated negative electrons and positive ions of atoms make up nearly ninety percent of all material in space, and plasma can be found in conditions of the atmosphere, gaseous nebulae, interstellar hydrogen, and star interiors [11]. Electrons and positive or negative ions combine to form plasma, a gaseous mixture that can be either fully or partially ionized, similar to the sun or fluorescent lightbulbs. Plasma is classified into two types based on electron temperature in relation to other particles: Thermal and non-thermal (neutral and ionized). The temperature of massive particle and electron is about equal in a thermal plasma (thermal equilibrium), but heavy particles are noticeably warmer than electrons in a non-thermal plasma [12]. Chemical synthesis, which uses hazardous substances as oxidizing/reducing agents, is the primary method for producing nanoparticles. To lessen nanomaterial toxicity, alternative "green" strategies must be developed. Plasma technologies have played a significant role in nanomaterial production [13]. Given their tiny size and wide surface area, core-shell nanoparticles combine many intrinsic features that make them attractive candidates for theranostic medicines. However, the screening and optimization of synthesis conditions, or their monitored synthesis, are frequently challenging and labor-intensive. Conventional bulk materials are unable to interact with biological systems in the same way as nanoparticles because of their small size and huge surface area. Core-shell nanoparticles combine two distinct materials to provide access to a broader range of features. Through this, two materials with different functions can be effectively coupled to treat a disease, which makes these core-shell nanoparticles intriguing candidates for theranostic applications [14]. Gold nanoparticles (Au NPs) have become more popular in bionanotechnology due to their unique qualities and variety of surface features. Au NPs are a useful substrate for nano biological assemblies that include oligonucleotides, antibodies, and proteins because of their ease of functionalization. Au-NPs bioconjugates, which have grown in popularity, are also being used to create novel biomaterials for biomedical research [15]. Because of their versatility, Au NPs have been useful in several biomedical applications. The adhesion of the sample may cause variations in the resonance of the surface Plasmon, Oxidation-Reduction reactions and conductivity of gold NPs, resulting in detectable signals for diagnostic purposes. A large number of biomedical applications employ Au NPs due to their greater living compatibility and ability for generate minuscule investigations for the study to cancerous cells. Au NPs can also accumulate in cancerous cells and reveal the specific cell and cell receptor's cytotoxicity [15, 16]. Various characteristics of nanoparticles and cellular interactions can be linked to the biocidal activities of Cr_2O_3 NPs. Due to their small size, nanoparticles typically enter cells easily and produce reactive oxygen species (ROS), which causes oxidative stress and eventually kills living cells. Apart from causing oxidative stress, reactive oxygen species (ROS) can also interact with enzymes, organelles, and cellular machinery. Moreover, the rough surface and surface flaws of the nanoparticles might lead to intracellular content leakage, which can cause harm to cells. In addition, intracellular damage could result from the intracellular production of Cr in the cellular medium [17]. Among the most popular cancer chemotherapeutic medicines are taxanes, which include the synthetic derivatives Taxol®, Anzatax®, and Paxene®. Taxanes primarily target β-tubulin found in polymerized microtubules. Taxanes have the ability to influence a variety of cancer biology pathways and processes, including angiogenesis, apoptosis, and the stability of regulatory proteins involved in mitosis. On the other hand, makes it possible to improve the effec-

tiveness of these medications and get around drug resistance mechanisms. However, significant adverse consequences may occur following treatment, such as bradycardia, myalgia/arthralgia, peripheral neuropathy, vomiting, nausea, diarrhea, alopecia, neutropenia, leukopenia, and hypersensitive responses [18]. *Thymus vulgaris*, a gentle member of the Lamiaceae family and a relative of the original oregano genus, is a medicinal herb. Common thyme (*Thymus vulgaris*) essential oil contains 20–54 percent thymol. Thyme has historically been used as medicine to treat wounds and shield wounded body parts. Prior to the discovery of contemporary pharmacological antibiotics. This plant species has recently been the subject of extensive clinical investigation, which has been reported by numerous universes. It appears to have very powerful antifungal, antioxidant, antibacterial, insecticidal, and antiplatelet properties. The majority of crude extract activities are typically obtained from Omani plants for medicinal purposes [19]. In this studies, The use of Green-plasma jet scheme to produced Cr Au core shell nanoparticles exhibit improved antioxidant activity due to the presence of phytomolecules from plant leaf extract on their surface, as shown by FTIR, XRD and SEM data and the calculate the cellular toxicity of those manufactured Nano-materials when combined with taxanes chemotherapy, by using aqueous solution from Core Shell nanomaterials with chemotherapy on MDA cancer cells line, my research goal was trying to kill cancer cells without affecting normal cells by Reducing the cytotoxicity of core shell nanoparticles with thymus vulgaris leaf extract with chemotherapy by application on the MDA breast cancer cell lines.

2. Materials and methods

2.1 *Thymus vulgaris*

Thymus vulgaris extraction obtained the Plant material of *Thymus vulgaris* L. from Amman/Jordan. The *Thymus vulgaris* plant was ground and stored at room temperature the needed. An aqueous extract was prepared by adding 350 milliliters of ethanol (80 percent) to 50 grams of powdered Thyme in a Soxhelt the extraction unit of production. The extraction process was then carried out for a period of twelve hours at 40 degrees Celsius using a Vacuuming Rotary Vaporizer, as well as at 35 degrees Celsius [20]. The extract was then taken and put into a cylindrical flask with 200 cm^3 of distilled water. The mixture was then placed in an electric oven at 35 degrees Celsius until the extract was produced [21].

2.2 Preparation of the chemical solution

The first chemical solution is a Salt of Chromium nitrate $CrNO_3$, with molecular weight 400,15 g/mol and with 2 mM concentration from it prepared as a core. The other salt which considered as shell was with 0.5 mM concentration from Aqueous gold tetrachloride salts with chemical formula ($AuCl_4$•$3H_2O$) and molecular weight 393.83 g/mol. The necessary weight can be computed using equation (1) [22].

$$\text{Concentration}\left(\frac{\text{mol}}{\text{liter}}\right) = \frac{\text{mass (g)}}{\text{Molecular weight}\left(\frac{\text{g}}{\text{mol}}\right)\times\text{Volume(liter)}} \quad (1)$$

2.3 Preparation of nanoparticles thyme extraction with Cr Nps as core and use gold for core-shell Nps

Synthesized Chrome:gold Core-Shell nanoparticles, Chrome:gold nanoparticles were first produced in scheme consist of a glass tube with 1 mm diameter in width and fix vertically by holder with argon gas was used with voltage (20 kV), the Argon gas flow meter is 3 L/min, and 1 cm was the length of the plasma between the two electrodes as shown in Fig. 1. Later the preparation of the 8 mM Chromium nitrate $CrNO_3$ salt solution mixed with 2 mM of thyme extraction liquid as show in Fig. 2 (A). After the created form was exposed to a chemical solution for 17 minutes to prepare a (2:8) as a core, the coloring of the chrome solution changed to a dark olive color, as shown

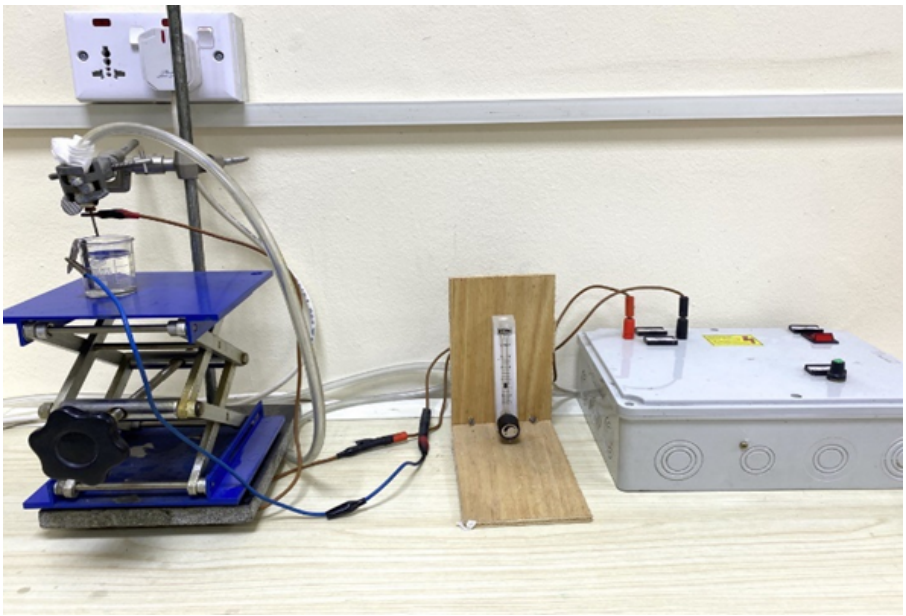

Figure 1. Plasma jet scheme.

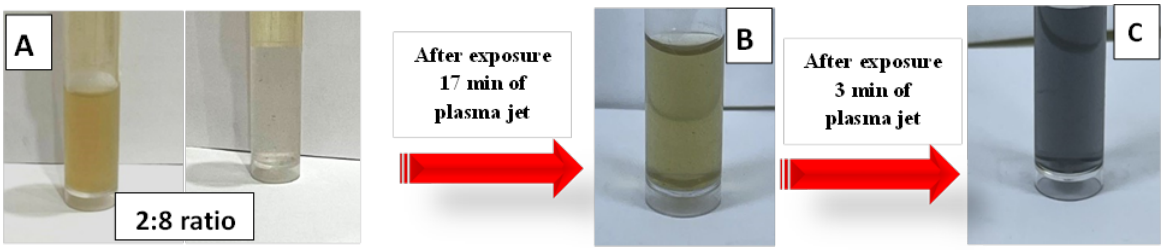

Figure 2. Synthesized core-shell Nps (A) Thyme extraction + $Cr(NO_3)_3$ salt (B) Core (Cr) NPs (C) Core:Au NPs.

in figure 2 (B), as a result of the process of reaction. The beaker containing 10 mL of the solution will have the created form on it at a distance of 4 cm from the surface of the liquid. Subsequently, combine 2 milliliters of Cr Nanoparticles (core) with 8 milliliters of Aqueous gold tetrachloride salts with chemical formula ($AuCl_4$•$3H_2O$) them put in a flask and irradiated to cold plasma system for 3 min to produced a 2:8 ratio of Cr:Au NPs in the figure 2 (C).

2.4 Preparation and exposure of cell line by Cr:Au core shell nanoparticlase for *in vitro* study

The human breast cancer cell line MDA was cultured in RPMI- medium which contain 100 units/mL penicillin, 10 percentage of (FBS) fetal bovine serum with 100 gram/mL streptomycin. Subsequent cell spreading, the microtiter-plate 96 (12×8) well which use to grow the cells with range of 10000 cells/well. The study was conducted at the Center for Research for Al-Nahraein University of bio-technology. The investigation went like this: The human cancerous breast MDA cell line was grown in RPMI-1640 media supplemented with 10 percent fetal bovine serum (FBS), 100 grams per milliliter of streptomycin, and 100 units/mL penicillin. The microtiter plate, consisting of 96 wells, was utilized for seeding about 10000 cells/well) after cell dispersal. At 37 °C they were incubated. The Cr:Au core shell nanomaterial were 100%, 50% and 25% which combined with chemo therapy in 25 µg, 50 µg and 100 µg. There were three attempts, and each time the attempt was exposed to Cr:Au core shell NPs with chemo therapy for twelve, forty-eight, and seventy-two hours at 37 degrees Celsius. After every period of incubation, 100 µL/well of crystal violet stain was applied, and those cells had been incubated for an additional twenty minutes at 37 degrees Celsius. In the end, a microplate reader was used to read the results at the wavelength of 580 nm. The ratio for inhibition rate of breast cancer cells line was estimated. To determine the rate of cell inhibition used equation (2) [23].

$$\text{Rate of Growth Inhibition } (G.I)\% = \frac{\text{control cells} - \text{treated cells}}{\text{control cell}} \times 100\% \quad (2)$$

3. Result and discussions

3.1 UV-visible spectrum of core Cr and Cr:Au core-shell NPs combine with taxans chemo therapy

The Cr:Au core-shell NPs that were formed by system of the Argon jet scheme and the reaction happen between the thyme extraction and chromium salt after that formed core NPs that were formed by using the Argon jet system and the reaction happen between the core and gold salt solutions to generation of core-shell by these system, the color of solutions are change and this change considered indicate to formation of Nps during mixing of the chromium and gold salts solutions. Surface plasmon resonance (SPR) gives the particles metal another color when the diameter of particle becomes close to a nanometer, as in the chromium and gold state. The generation of the Cr:Au core-shell nano-particles has been describe by the use of spectral scanning device at visible light wavelengths and UV-visible of the spectral absorption of with colloidal Core NPs with various ratio between core-shell (0:10, 1:9, 2:8, and 3:7). Where the UV examination result peak for Cr Nps only was 418 nm as show in figure 3 and the peaks were $(310 - 550)$ nm respectively and considered as a function of core ratio are appear in figure 4. Furthermore, the result confirm the presence of Cr:Au NPs at a ratio 2:8 with a circle-shaped and compact with results from other examine using Mie thesis to simulate Cr: Au core shell nano-particles light scattering spectra as appear in figure 5.

3.2 X-Ray diffraction (XRD)

The dry Cr NPs create by the Aragone jet method had altered XRD patterns that showed the Bragg reflection, a sign of the Cr NPs' fcc structures. The XRD CrNPs' spectra are displayed in figure 6. The Chrome peaks at 2θ of (28.49, 42.19 and 56.10) based to powder diffraction standard (PDF) leflet Cr stander 01-088-2323, the outcome showed that every peak appeared to be directed towards chrome and gold core shell. Using the ratios, the XRD results for the

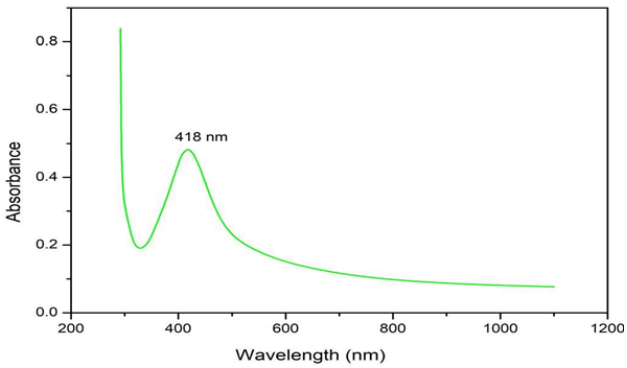

Figure 3. The absorption spectrum of Cr nanoparticles formed by plasma jet scheme, showing the one of ultraviolet-visible spectrum peak.

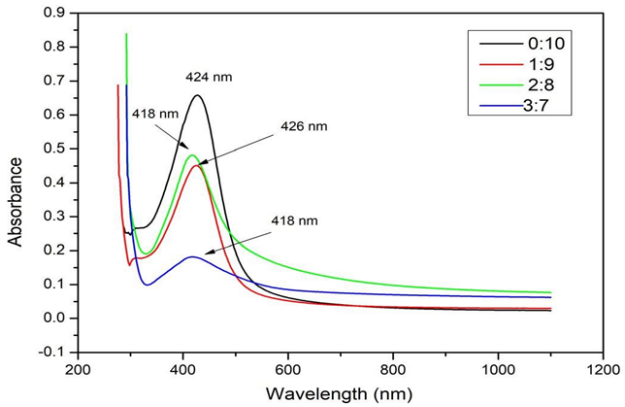

Figure 4. The absorption spectrum of core (Cr:thyme) nanoparticles formed by plasma jet scheme, showing the various ratios' effects on the ultraviolet-visible spectrum band.

core-shell were calculate. The angles peaks for a Cr with thyme extraction as a core was (28.49, 42.19 and 56.10) identical to the (111), (115), and (125) respectively, for Au (38.18, 44.4, 64.76 and 77.5) corresponding to the (111), (200), (220) and (311) planes, in figure 7. The diffraction style of peaks, as previously noted, cannot be reproduced in other types of material, indicating the purity and non-attendance of any more impurities in the produced sample [24].

3.3 Field emission (FE-SEM) scanning electron microscopy

Scanning electron microscopy using field emission, the morphological concepts of Cr:Au core shell NPs which scanned by atmospheric plasma jet schem. From image explanation of the FE-SEM (figure 8), core-shell NPs have sphere-shaped and also another particle same spot lighting. The diameter of the Cr:Au core-shell nanoparticles were discovered (80.78 – 102.34) nm. It is well known that the type of metal nanoparticles have a profound effect on visual and electric properties.

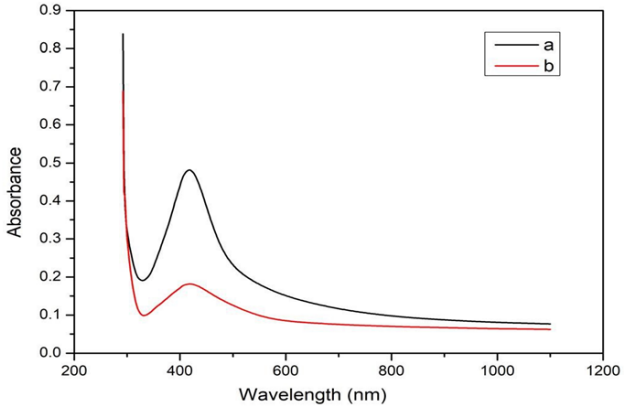

Figure 5. The absorption spectrum of core-shell nanoparticles formed by plasma jet scheme, showing (a) as a core in 2:8 ratio of thyme extraction to chrome and (b) as gold shell on the ultraviolet-visible spectrum band.

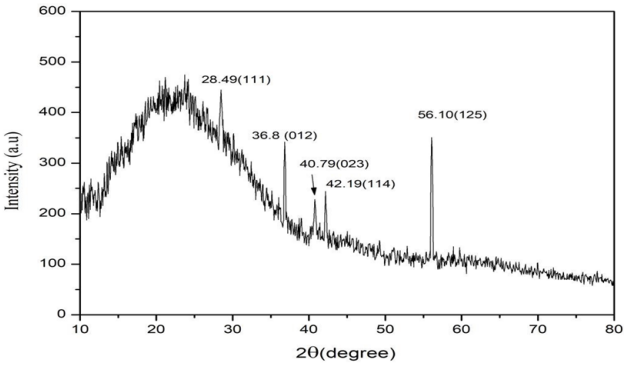

Figure 6. X-ray shapes of nanoparticles Cr Nps created by using plasma jet scheme as a core.

3.4 Transmission electron microscopy TEM

The core-shell structure of colloidal particles was revealed by the analysis of the observed TEM images. Particles were found to consist of a chrome core and a gold shell. TEM image showed that the mean particle size increases from (80.78 – 102.34) nm, which is in good agreement with predicted theoretical values. The produced Cr:Au core-shell nanoparticals was successfully used for preparation at 2:8 percentage. TEM analysis demonstrated that nanoparticles exhibited an approximate equi-axes shape with no sharp edges observed. Almost all the particles contained quite a few particles in the form of aggregated granules as show in figure 9.

3.5 Cytotoxicity breast cancer cells line and normal cells line

A range of series diluting the Cr:Au NPs combined with taxans chemo therapy in 25 µg, 50 µg and 100 µg varied ratio after effect 24, 48 and 72 hours from exposure have been used to assess the cytotoxicity of the in-vitro investigations against the Normal Rate embryonic cells line (REF) and the breast cancer cells line (MDA). After 24 hours the highest rate of toxicity for MDA breast cancer cell in 100% concentration of Chrome:gold core shell nanoparticles and Chrome:gold core shell nanoparticles combined with 25 µg, 50 µg, 100 µg of taxans

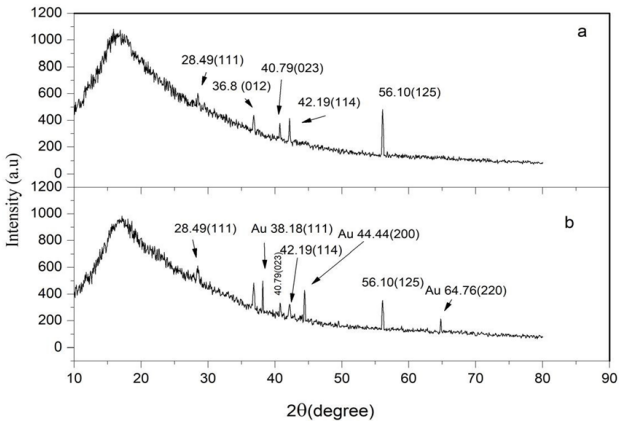

Figure 7. X-ray shapes of nanoparticles (NPs) created by using plasma jet scheme as an 2:8 ratio function (Cr:Au) core-shell NPs.

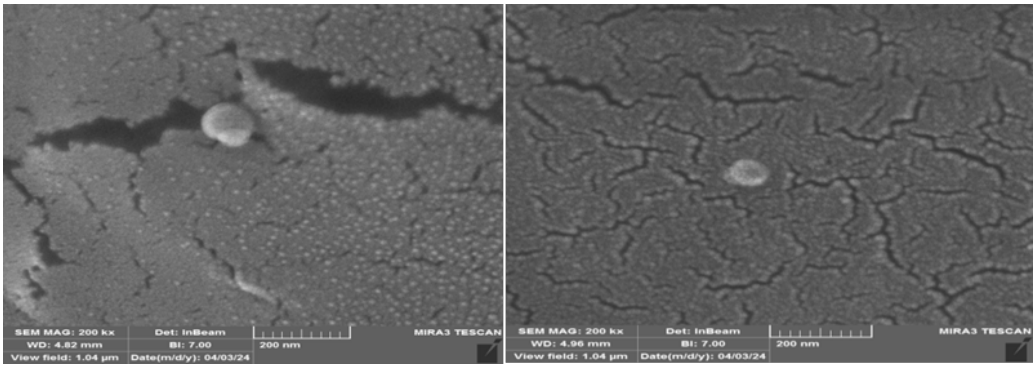

Figure 8. Images of FE-SEM to the Cr:Au core-shell NPs which prepared plasma jet scheme.

chemo therapy was (10.3 ± 3.2), (18.3 ± 4.1), (23.3 ± 3.5), (26.6 ± 2.5), the least amount of toxicity in 25% concentration of Chrome:gold core shell nanoparticles and Chrome:gold core shell nanoparticles combined with 25 µg, 50 µg, 100 µg of taxans chemo therapy was (5 ± 2), (10 ± 3), (14 ± 2), (18.3 ± 3.5) as shown in figures 10 and the maximum toxicity for the normal cells line (REF) in 100% concentration of Chrome:gold core shell nanoparticles and Chrome:gold core shell nanoparticles combined with 25 µg, 50 µg, 100 µg of taxans chemo therapy was (7.6 ± 1.5), (11.3 ± 1.5), (15 ± 1), (19.3 ± 1.5), the least amount of toxicity in 25% concentration of Chrome:gold core shell nanoparticles and Chrome:gold core shell nanoparticles combined with 25 µg, 50 µg, 100 µg of taxans chemo therapy was (2 ± 1), (5.6 ± 1.5), (9.3 ± 1.5), (12.3 ± 2.5) as shown in figures 11.

And after 48 hours the maximum rate of toxicity for MDA breast cancer cell in 100% concentration of Chrome:gold coreshell nanoparticles and Chrome:gold coreshell nanoparticles combined with 25 µg, 50 µg, 100 µg of taxans chemo therapy was (34.6 ± 4.1), (35.3 ± 2.8), (41.6 ± 2.08), (47.3 ± 2.5), the least amount of toxicity in 25% concentration of Chrome:gold coreshell nanoparticles and Chrome:gold coreshell nanoparticles combined with 25 µg, 50 µg, 100 µg of taxans chemo therapy was (22.6 ± 2.5), (25.6 ± 3.2), (32 ± 2.6), (37.6 ± 2.5). As shown in figures 12 and the maximum toxicity for the normal cells line (REF) in 100% concentration of Chrome:gold coreshell nanoparticles and Chrome:gold coreshell nanoparticles combined with 25 µg, 50 µg, 100 µg of taxans chemo therapy was (23 ± 1), (25 ± 1), (29.3 ± 2.08), (33.6 ± 1.5) ,the least amount of toxicity in 25% concentration of Chrome:gold coreshell nanoparticles and Chrome:gold coreshell nanoparticles combined with 25 µg, 50 µg, 100 µg of taxans chemo therapy was (16.3 ± 1.5), (20 ± 2), (24 ± 2), (29 ± 1) as shown in figures 13.

And after 72 hours the maximum rate of toxicity for MDA breast cancer cell in 100% concentration of Chrome:gold core shell nanoparticles and Chrome:gold core shell nanoparticles combined with 25 µg, 50 µg, 100 µg of taxans chemo therapy was (36 ± 3), (41 ± 2), (47.3 ± 2.5), (56 ± 3), the least amount of toxicity in 25% concentration of Chrome:gold core shell nanoparticles and Chrome:gold core shell nanoparticles combined with 25 µg, 50 µg, 100 µg of taxans chemo therapy was (24 ± 3.6), (33.6 ± 4.5), (37.6 ± 2.5), (42.6 ± 3.5) as shown in figures 14 and the maximum toxicity for the normal cells line (REF) in 100% concentration Chrome:gold core shell nanoparticles and

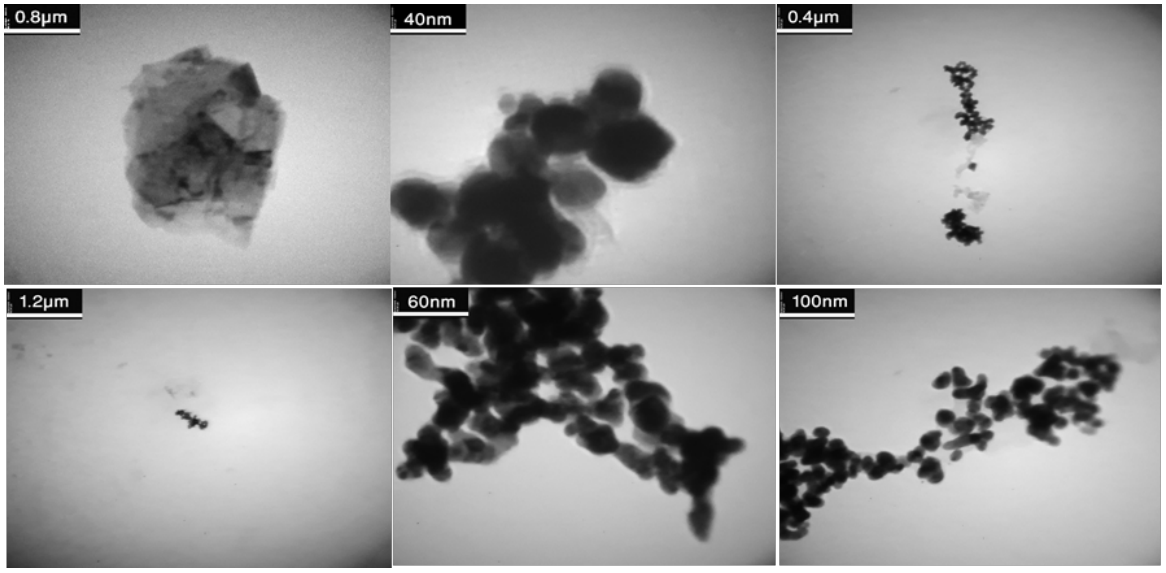

Figure 9. Images of TEM to the Cr:Au core-shell NPs which prepared plasma jet scheme.

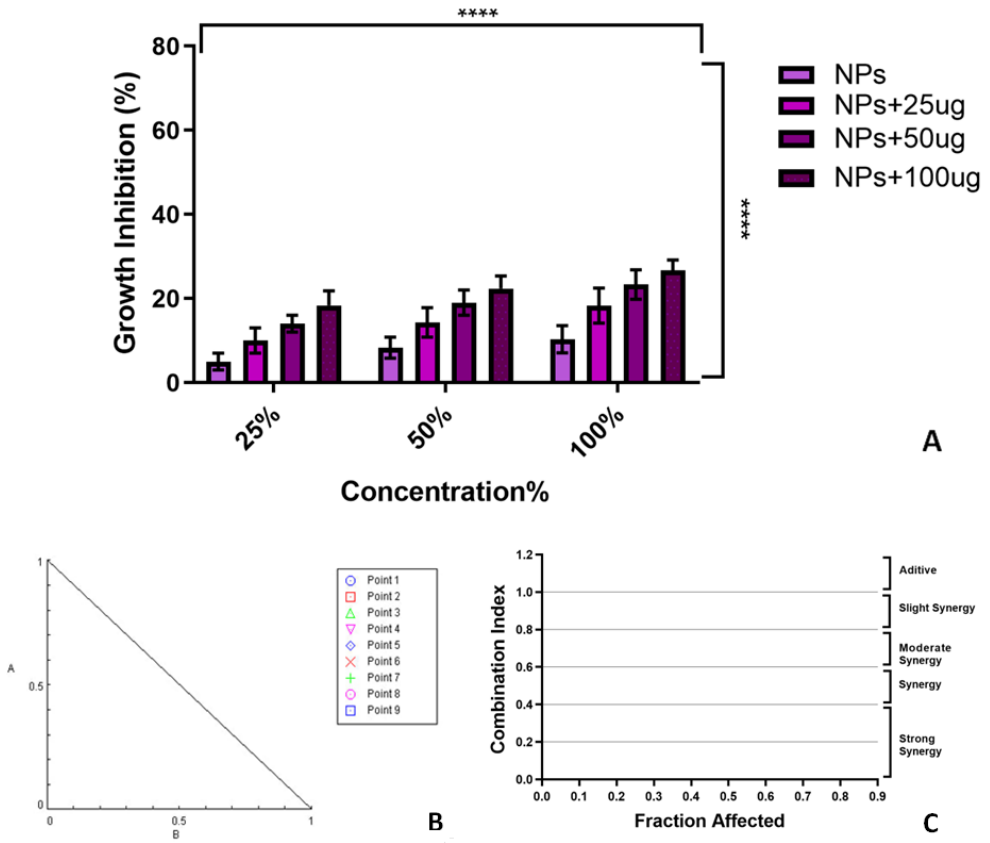

Figure 10. Cytotoxicity effect of the breast cancer cells line (MDA) of Cr:Au NP combined with taxans chemo therapy after 24 hours of incubating: (A) growth suppression, (B) iso-bologram, and (C) combinations index.

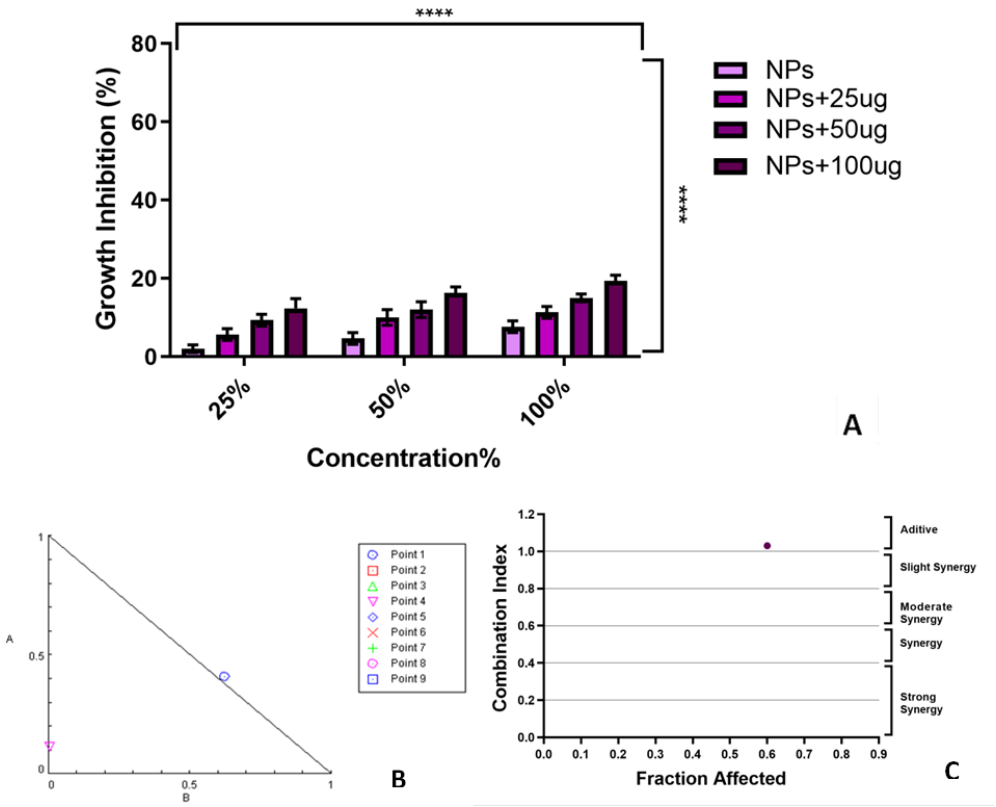

Figure 11. Cytotoxicity effect of the normal cells line (REF) of Cr:Au NP combined with taxans chemo therapy after 24 hours of incubating: (A) growth suppression, (B) iso-bologram, and (C) combinations index.

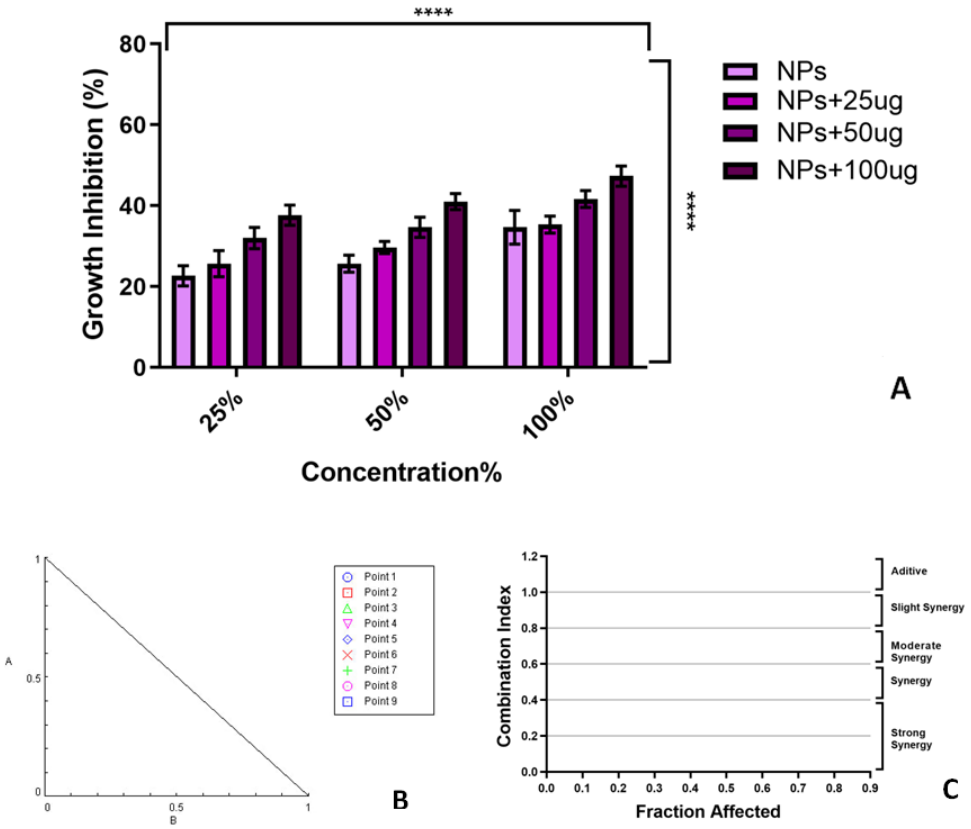

Figure 12. Cytotoxicity effect of the breast cancer cells line (MDA) of Cr:Au NP combined with taxans chemo therapy after 48 hours of incubating: (A) growth suppression, (B) iso-bologram, and (C) combinations index.

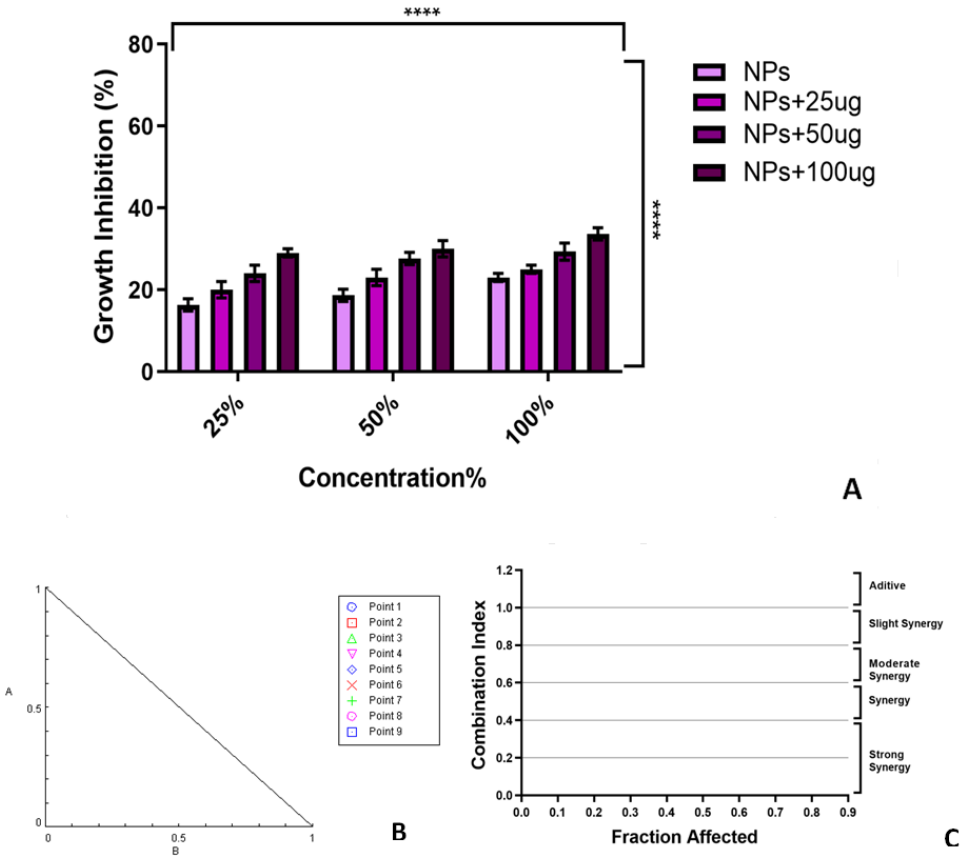

Figure 13. Cytotoxicity effect of the normal cells line (REF) of Cr:Au NP combined with taxans chemo therapy after 48 hours of incubating: (A) growth suppression, (B) iso-bologram, and (C) combinations index.

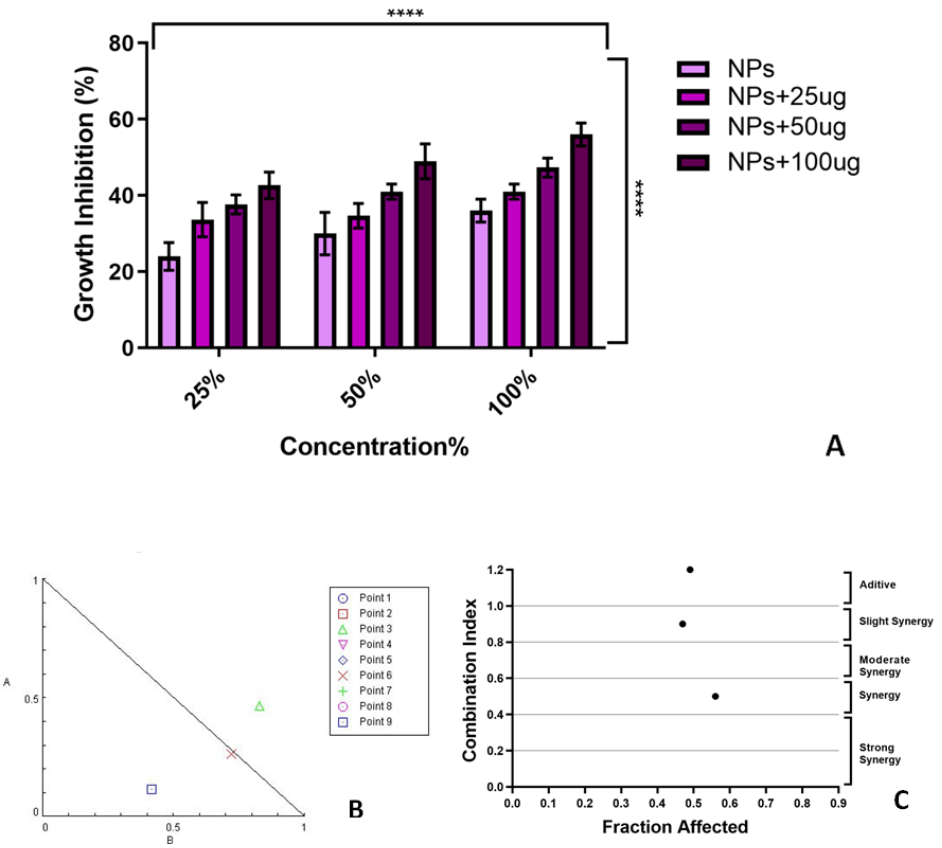

Figure 14. Cytotoxicity effect of the breast cancer cells line (MDA) of Cr:Au NP combined with taxans chemo therapy after 72 hours of incubating: (A) growth suppression, (B) iso-bologram, and (C) combinations index.

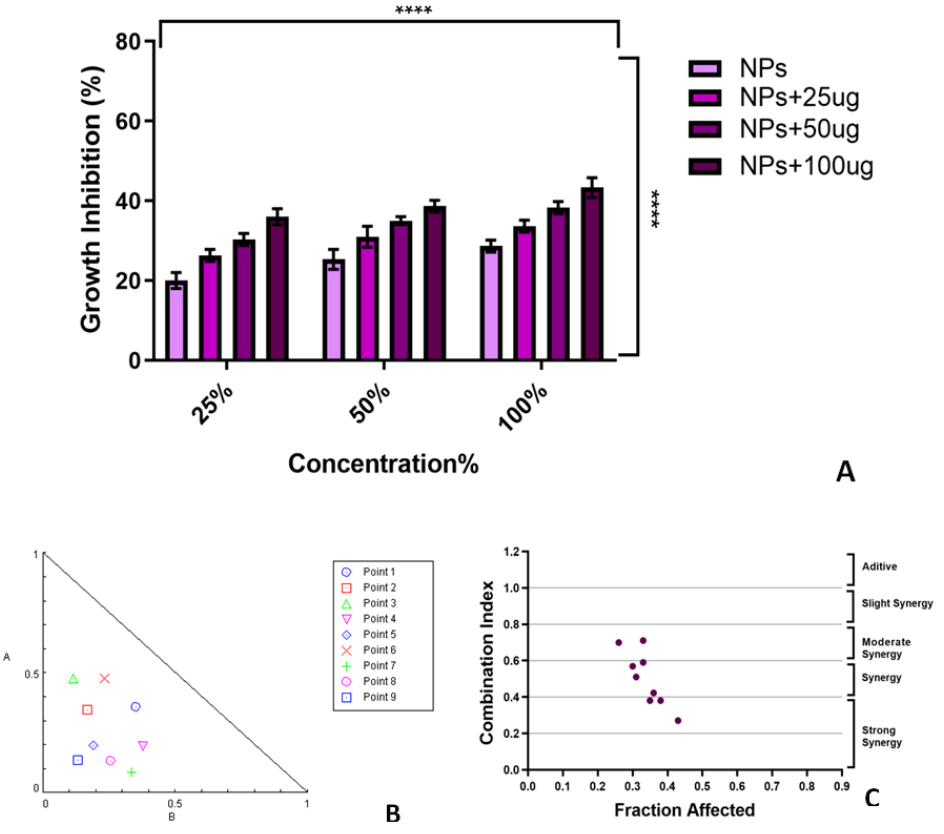

Figure 15. Cytotoxicity effect of the normal cells line (REF) of Cr:Au NP combined with taxans chemo therapy after 72 hours of incubating: (A) growth suppression, (B) iso-bologram, and (C) combinations index.

Chrome:gold core shell nanoparticles combined with 25 µg, 50 µg, 100 µg of taxans chemo therapy was (28.6 ± 1.5), (33.6 ± 1.5), (33.6 ± 1.5), (43.3 ± 2.5), the least amount of toxicity in 25% concentration of Chrome:gold core shell nanoparticles and Chrome:gold core shell nanoparticles combined with 25 µg, 50 µg, 100 µg of taxans chemo therapy was (20 ± 2), (33.6 ± 1.5), (38.3 ± 1.5), (43 ± 2.5) as shown in figures 15.

When MDA cell line is exposed to Cr:Au core shell nanoparticles combination with taxans chemotherapy in different concentration (25 µg, 50 µg, 100 µg) there is no synergism effect after 24, 48 hrs of incubation, while after 72 hrs of incubation present synergism effect and the growth inhibition increase with increasing concentration of Cr:Au core shell nanoparticles combination with taxans chemotherapy more than when expose to Cr:Au NPs alone, these results are consistent with some researches [25, 26]. While in the same condition ,concentrations and exposed appear strong synergism effect after 72 hrs of incubation and also no synergism effect after 24, 48 hrs of incubation in REF cell line.

4. Conclusion

In this study has describe that the Cr:Au core shell NPs create by using plasma-jet scheme which combined with taxans chemotherapy in different concentration (25 µg, 50 µg, 100 µg) more inhibition growth of breast cancer in the MDA cell-line. It is conceder a familiar, nontoxic, inoffensive and rapid method to make nanomaterial use plasma-jet scheme method. The procedure, which used thyme extraction with of hydrous salts of $Cr(NO_3)_3$ Chromic Nitrate as a core and use aqueous salts of ($HAuCl_4$•$4H_2O$) gold tetrachloride as a shell, produces Cr:Au core-shell Nps with safe a great level of efficiency. UV-visible spectral that were gainted appear that band of absorbance in 540 nm, which take as a indicator of Cr:Au NPs' plasmon resonance at the surface. According to the X-ray diffraction results, the sample created at a ratio of 2:8 appears to have produced the better results. 2 from core and 8 from Au shell where the diffraction form appear it has a large number of values by 4-values. FE-SEM give dateile regarding the shape of Cr:Au coreshell NPs. In particular, the differences in particle sizes between $84.78 - 106.72$ nm, which nearly identical, to the result of (XRD) research. Because these properties of the NPs including size, shape, and surface charge have various effects on their interactions with living cells such as cellular uptake, localization and cytotoxicity [27]. Small NPs have a high probability to be internalized by passive uptake than large one. In addition, culture media with/without FBS have been reported to affect the size stability in vitro systems, showing that NPs aggregated in a high-ionic-strength medium such as PBS or RPMI-1640 solution [28]. The Cr:Au core shell NPs prepared by plasma jet scheme give synergism effect that increase the cytotoxicity to MDA cell line for breast cancer, according to the interpretation, it is believed that Cr:Au NPs was pragmatic in culture media, and induced ROS production in a dose-dependent manner. Thus, this is an interesting, leading that complex of MNPs, a chemotherapeutic agent and FBS may increase effect on interactions such as cellular uptake via alternative endocytosis pathways [29]. This study opens the entrance for the use of Cr:Au core-shell NPs compined with taxans chemotherapy to considered as a more faster, detected cancer cells and effected therapy to kill of the breast cancer in futurity [30].

Authors Contribution
Authors have contributed equally in preparing and writing the manuscript.

Availability of data and materials
The datasets generated (or analyzed) during the current study are available from the corresponding author on reasonable request.

Conflict of interests
The authors declare that they have no known competing financial interests or personal relationships that could have appeared to influence the work reported in this paper.

References

[1] X. Fang, J. Cao, and A. Shen. "Advances in anti-breast cancer drugs and the application of nano-drug delivery systems in breast cancer therapy. ". *Journal of Drug Delivery Science and Technology*, page 101662, 2020.
DOI: https://doi.org/10.1016/j.jddst.2020.101662.

[2] S. J. Han, Q. Q. Guo, T. Wang, Y. X. Wang, Y. X. Zhang, F. Liu, Y. X. Luo, J. Zhang, Y. L. Wang, Y. X. Yan, X. X. Peng, Y. X. Yan, R. Ling, and Y. He. "Prognostic significance of interactions between ER alpha and ER beta and lymph node status in breast cancer cases.". *Asian Pac J Cancer Prev*, **14**:6081–4, 2013.
DOI: https://doi.org/10.7314/apjcp.2013.14.10.6081.

[3] J. A. de la Mare, L. Contu, M. C. Hunter, B. Moyo, J. N. Sterrenberg, K. C. Dhanani, L. Z. Mutsvunguma, and A. L. Edkins. "Breast cancer: current developments in molecular approaches to diagnosis and treatment.". *Recent Pat Anticancer Drug Discov*, **9**:153–75, 2014.
DOI: https://doi.org/10.2174/15748928113086660046.

[4] M. Wielsøe, S. Gudmundsdottir, and E. C. Bonefeld-Jørgensen. "Reproductive history and dietary habits and breast cancer risk in Greenlandic Inuit: a case control study. ". *Public Health*, **137**:50–58, 2016.
DOI: https://doi.org/10.1016/j.puhe.2016.06.016.

[5] A. Florescu, E. Amir, N. Bouganim, and M. Clemons. "Immune therapy for breast cancer in 2010-hype or hope?". *Current Oncology*, **18**, 2011.
DOI: https://doi.org/10.3747/co.v18i1.623.

[6] M. Mohammed, J. Syeda, K. Wasan, and E. Wasan. "An overview of chitosan nanoparticles and its application in non-parenteral drug delivery.". *Pharmaceutics*, **9**:53, 2017.
DOI: https://doi.org/10.3390/pharmaceutics9040053.

[7] X. Kang, H. Chen, S. Li, L. Jie, J. Hu, X. Wang, J. Qi, X. Ying, and Y. Du. "Magnesium lithospermate B loaded PEGylated solid lipid nanoparticles for improved oral bioavailability.". *Colloids and Surfaces B: Biointerfaces*, **161**:597–605, 2018.
DOI: https://doi.org/10.1016/j.colsurfb.2017.11.008.

[8] A. E. Nadimi, S. Y. Ebrahimipour, E. G. Afshar, S. K. Falahati-pour, Z. Ahmadi, R. Mohammadinejad, and M. Mohamadi. "Nano-scale drug delivery systems for antiarrhythmic agents.". *European Journal of Medicinal Chemistry*, **157**:1153–1163, 2018.
DOI: https://doi.org/10.1016/j.ejmech.2018.08.080.

[9] L. E. Van Vlerken and M. M. Amiji. "Multi-functional polymeric nanoparticles for tumour-targeted drug delivery. ". *Expert Opinion on Drug Delivery*, **3**:205–216, 2006.
DOI: https://doi.org/10.1517/17425247.3.2.205.

[10] A. Ghaffari, D. Dorranian, and A. Khajehnezhad. "Role of nitrogen and silver compounds in photocatalytic properties of carbon nanoparticle.". *Fullerenes, Nanotubes and Carbon Nanostructures*, **33**:1–12, 2024.
DOI: https://doi.org/10.1080/1536383X.2024.2392032.

[11] F. F. Chen. "Introduction to plasma physics and controlled fusion. ". *Plenum Press*, pages 19–51, 1984.

[12] D. B. Graves. "The emerging role of reactive oxygen and nitrogen species in redox biology and some implications for plasma applications to medicine and biology.". *J Phys D: Appl Phys*, **45**:263001, 2012.
DOI: https://doi.org/10.1088/0022-3727/45/26/263001.

[13] K. Ostrikov, E. C. Neyts, and M. Meyyappan. "Plasma nanoscience: From nano-solids in plasmas to nanoplasmas in solids. ". *Adv Phys*, **62**:113–224, 2013.
DOI: https://doi.org/10.1080/00018732.2013.808047.

[14] E. K. Lim, T. Kim, S. Paik, S. Haam, Y. M. Huh, and K. Lee. "Nanomaterials for theranostics: recent advances and future challenges.". *Chem Rev*, **115**:327–394, 2015.
DOI: https://doi.org/10.1021/cr300213b.

[15] M. A. Qaeed, A. Hendi, A. S. Obaid, A. A. Thahe, A. M. Osman, A. Ismail, A. Mindil, A. A. Eid, F. Aqlan, N. M. A. Osman, A. AL-Farga, et al. "The effect of different aqueous solutions ratios of Ocimum basilicum utilized in AgNPs synthesis on the inhibition of bacterial growth.". *Scientific Reports*, **13**:5866, 2023.
DOI: https://doi.org/10.1038/s41598-023-31221-7.

[16] I. I. Jaleel, A. Obaid, H. H. Ali, and Khalil T. Hassan. "One-step biosynthesis of gold nanoparticles using natural reductive extracts.". *Nano Biomedicine and Engineering*, **12**:331–337, 2020.
DOI: https://doi.org/10.5101/nbe.v12i4.p331-337.

[17] A. S. Obaid, Khalil T. Hassan, Omar M. Hassan, H. Hussein Ali, Ibraheem J. Ibraheem, Thaer A.r Salih, Ban H. Adil, and Maha M. Almoneef. "*in-vitro* antibacterial, cytotoxicity, and anti-prostate cancer effects of gold nanoparticles synthesized using extract of desert truffles (tirmania nivea).". *Materials Chemistry and Physics*, **301**:127673, 2023.
DOI: https://doi.org/10.1016/j.matchemphys.2023.127673.

[18] L. Mosca, A. Ilari, F. Fazi, Y. G. Assaraf, and G. Colotti. "Taxanes in cancer treatment: Activity, chemoresistance and its overcoming. ". *Drug Resistance Updates*, **54**:100742, 2021.
DOI: https://doi.org/10.1088/0022-3727/45/26/263001.

[19] O. M. Hassan, I. J. Ibraheem, B. H. Adil, A. S. Obaid, and T. A. Salih. "Synthesis of Silver Nanoparticles by ecofriendly nvironmental method using Piper nigrum, Ziziphus spina-christi, and Eucalyptusglobulus extract.". *Journal of Physics: Conference Series*, **1530**: 012139, 2020.
DOI: https://doi.org/10.1088/1742-6596/1530/1/012139.

[20] C. E. DeSantis, J. Ma, A. Goding Sauer, L. A. Newman, and A. Jemal. "Breast cancer statistics, 2017, racial disparity in mortality by state.". *CA Cancer J. Clin*, **67**:439–448, 2017.
DOI: https://doi.org/10.3322/caac.21412.

[21] J. O'Shaughnessy. "Extending survival with chemotherapy in metastatic breast cancer.". *Oncologist*, **10**:20–29, 2005.

[22] B. H. Adil, K. A. Aadim, and M. A. Khalaf. "Synthesis and spectroscopic characterization of platinum nanoparticles by plasma jet method.". *Int J Nanosci*, **20**:2150030, 2021.
DOI: https://doi.org/10.1142/S0219581X21500307.

[23] M. S. Mohammed, B. H. Adil, A. S. Obaid, and A. M. Al-Shammari. "Plasma Jet Prepared Gold and Silver Nanoparticles to Induce Caspase-Independent Apoptosis in Digestive System Cancers. ". *Materials Science Forum*, **1050**:51–63, 2022.
DOI: https://doi.org/10.1142/S0219581X21500307.

[24] A. S. Obaid, M. A. Mahdi, and Z. Hassan. "Nanocoral PbS thin film growth by solid-vapor deposition.". *Optoelectronics and Advanced Materials, Rapid Communications*, **6**:422–424, 2012.
DOI: https://doi.org/10.1051/0004-6361:20020975.

[25] B. H. Adil, A. S. Obaid, M. M. Al-Halbosiy, and H. H. Murbat. "Use of cold plasma in the synthesis of gold nanomaterials for parasitic leishmaniasis treatment.". *Int. J. Plasma Environ. Sci. Technol*, **14**, 2020.
DOI: https://doi.org/10.34343/ijpest.2020.14.e02005.

[26] M. S. Jabir, A. M. Al-Shammari, Z. O. Ali, S. Albukhaty, G. M. Sulaiman, S. F. Jawad, S. S. Hamzah, et al. "Combined oncolytic virotherapy gold nanoparticles as synergistic immunotherapy agent in breast cancer control. ". *Sci Rep*, **13**:16843, 2023.
DOI: https://doi.org/10.1038/s41598-023-42299-4.

[27] L. Shang, K. Nienhaus, and G. U. Nienhaus. "Engineered nanoparticles interacting with cells: size matters. ". *J Nanobiotechnol*, **12**:5, 2014.
DOI: https://doi.org/10.1186/1477-3155-12-5.

[28] H. T. R. Wiogo, M. Lim, V. Bulmus, J. Yun, and R. Aml. "Stabilization of magnetic iron oxide nanoparticles in biological media by fetal bovine serum (FBS). ". *Langmuir*, **27**:843–850, 2011.

[29] T. L. Moore, L. Rodriguez-Lorenzo, V. Hirsch, S. Balog, D. Urban, C. Jud, N. Rothen-Rutishauser, M. Lattuada, and A. Petri-Fink. "Nanoparticl coolidal stability in cell culture media and impact on cellular interactions.". *Chem Soc Rev*, **44**:6287–6305, 2015.
DOI: https://doi.org/10.1039/C4CS00487F.

[30] K. Kojima, S. Takahashi, S. Saito, Y. Endo, T. Nittami, T. Nozaki, R. C. Sobti, and M. Watanabe. "Combined effects of Fe_3O_4 nanoparticles and chemotherapeutic agents on prostate cancer cells *In Vitro*. ". *Applied Sciences*, **8**:134, 2018.
DOI: https://doi.org/10.3390/app8010134.